Pharm Res (2013) 30:387–401
DOI 10.1007/s11095-012-0879-1

RESEARCH PAPER

Beyond Glass Transitions: Studying the Highly Viscous and Elastic Behavior of Frozen Protein Formulations Using Low Temperature Rheology and Its Potential Implications on Protein Stability

Jian Hua Gu • Alice Beekman • Tian Wu • Deirdre Murphy Piedmonte • Priti Baker • Michael Eschenberg • Michael Hale • Merrill Goldenberg

Received: 11 April 2012 / Accepted: 27 August 2012 / Published online: 16 October 2012

ABSTRACT

Purpose A novel application of oscillatory shear rheology was used to directly monitor global phase behavior of protein formulations in the frozen state and study its correlation with physical instability of frozen protein formulations.

Methods Oscillatory rheology was used to measure changes in rheological parameters and to identify mechanical softening temperature (Ts*) and related properties of an IgG2 mAb formulation. Rheological measurements were compared to DSC/MDSC. Physical stability of IgG2 formulations was monitored by SE-HPLC.

Results Rheological parameters and Ts* of an IgG2 formulation were sensitive to physical/morphological phase changes during freezing and thawing. Ts* of the frozen formulation was a function of concentration of protein and excipient. Complex modulus, G*, and phase angle, δ, for IgG2 at 70 mg/mL in a sucrose-containing formulation showed the system was not completely frozen at −10°C, which correlated to stability data consistent with ice-induced protein aggregation.

Conclusions We report the first application of oscillatory shear rheology to study phase behavior of IgG2 in a sucrose-containing formulation and its correspondence with physical stability not explained by glass transition (Tg'). We provide a mechanism and data suggesting that protein instability occurs at the ice/water interface.

KEY WORDS frozen state · glass transition · ice-induced protein aggregation · oscillatory rheology · protein stability

ABBREVIATIONS

DSC	differential scanning calorimetry
FB	formulation buffer
G*	complex modulus
G'	storage/elastic modulus
G"	loss/viscous modulus
HMWS	high molecular weight species
mAb	monoclonal antibody
MDSC	modulated differential scanning calorimetry
SE-HPLC	size exclusion high performance liquid chromatography
Tanδ	G"/G' or ratio of energy lost to energy stored at the peak stress during the mechanical cycle
Tg'	glass transition temperature of maximally freeze-concentrated amorphous phase in frozen aqueous solutions
Tg"	glass transition temperature of the amorphous phase whose concentration lies between the nominal concentration of the given solution and the concentration

Electronic supplementary material The online version of this article (doi:10.1007/s11095-012-0879-1) contains supplementary material, which is available to authorized users.

J. H. Gu • A. Beekman • D. M. Piedmonte • P. Baker • M. Goldenberg (✉)
Drug Product Development
Process and Product Development, Amgen Inc.
MS 8-1-C, One Amgen Center Drive
Thousand Oaks, California 91320, USA
e-mail: mgoldenb@amgen.com

T. Wu
Pharmaceutical R&D
Small Molecule Process and Product Development, Amgen Inc.
Thousand Oaks, California 91320, USA

M. Eschenberg • M. Hale
Medical Sciences Biostatistics, Amgen Inc.
Thousand Oaks, California 91320, USA

	of the maximally freeze-concentrated amorphous phase
Ts*	onset softening temperature of maximally freeze-concentrated amorphous phase in frozen aqueous solutions
δ	phase angle

INTRODUCTION

Background on Freezing

To prevent chemical and physical degradation of protein drug substance and drug product, protein solutions are often subjected to freezing temperatures either during cold storage or freeze drying. However, these temperatures are not always benign. In many situations (e.g., clinical sites and walk-in freezers for storage of drug substance) frozen storage is done at −20°C with an actual temperature range of −10°C to −30°C, and therefore a detailed stability profile over that range of temperatures is needed. Freezing of protein solutions may lead to protein denaturation, and is also a major stress factor that must be overcome for the successful freeze-drying of proteins (1–3). During freezing or thawing, the physical environment of a protein formulation changes dramatically and can subject a protein to several potentially destabilizing and known stresses, including: cold denaturation (4–6), destabilization at the ice-water interface (7–10) and freeze-concentration effects (e.g., concentration of excipients beyond their solubility, or to a concentration destabilizing to the protein) (11,12).

Freezing of an aqueous solution deviates from basic freezing point depression theory, beginning with the ice formation process itself, which involves poorly controlled nucleation events. Observed freezing points are often well below the theoretical ones, a phenomenon known as supercooling. Because minute and often highly variable quantities of particulate contaminants influence the nucleation process, observed freezing temperatures vary as well. Since the freezing process can be irreproducible, studies of the frozen state are often conducted by observing the melting of a fully frozen (solidified) material. In practical terms of formulation, this problem of supercooling may be addressed by pre-staging the material at a very low temperature to solidify it before storage at a higher subzero temperature.

Beyond the matter of supercooling, additional questions exist about the state of the protein and co-solutes at the various subzero temperatures. Often solution components do not crystallize out at the theoretical freezing point or even the eutectic point. Instead, the water gradually freezes as the temperature drops and the solutes become freeze concentrated in the remaining unfrozen solvent. This continues as the temperature drops, and the viscosity rises until water can no longer effectively diffuse from the concentrate and crystallize. A change in the heat capacity marks a transition to the glassy state, which is defined as the Tg' (glass transition temperature of maximally freeze-concentrated amorphous phase in frozen aqueous solutions). Glass formation also entraps liquid water that might otherwise have frozen. When the frozen material at a temperature well below the Tg' is warmed, various thermal events may occur such as crystallization of trapped water. Subambient DSC and MDSC (modulated differential scanning calorimetry) have been important tools for investigating the thermal behavior of frozen systems, such as the change of heat capacity at Tg' and exotherms and endotherms that accompany events such as crystallization or enthalpy recovery.

Besides DSC, additional analytical techniques such as microscopy(13), spectrometry(14–18) and certain types of rheology have been used to study the frozen state. While the spectroscopic approaches are useful, they apply to very local movements and changes at the molecular level. Rheological methods such as dynamic mechanical analysis (DMA) (19,20) and thermomechanical analysis (TMA) (20,21) have been used for characterization of bulk movement of frozen aqueous systems (19,20,22,23). These rheological methods are generally best suited to measurement of tensile and compressive resistance to deformation, and the results may be difficult to interpret in terms of the relative contributions of extensional and shear phenomena (21).

Rheological Properties

Shear rheology with instrumentation expressly designed for that purpose may be most relevant to the molecular mobility at low temperature. The shear modulus, G*, measures resistance to flow and deformation to force applied tangentially to a sample surface. While all of the moduli are interrelated, the shear modulus is probably most useful in situations where both liquid and solid behavior may occur, as during freezing and thawing. Furthermore, G* may be the most directly related to the ease with which molecules may move and diffuse through a medium as indicated, in general, by the Stokes-Einstein equation. When the deformation is reversible, the shear modulus can be thought of as an elastic resistance. However, where cohesive forces do not exist to restore the original structure, the deformation is irreversible and there is flow. In the classical Newtonian concept of viscosity, there is laminar flow parallel to the shearing force through the depth of the sample, and for each layer deeper into the sample, with a decreased flow velocity because of friction between the layers (24). For samples that are primarily "viscous" (i.e., experiencing resistance primarily due to friction during laminar flow), an appropriate type of rheological

measurement is "steady" in terms of direction (e.g., a measurement cone or plate that turns continuously in one direction).

However, if the sample is rigid or gel-like, a component of the measurement configuration will be compelled to break under steady shear: either the contact between the sample and the device (slippage), the sample (e.g., gel rupture) or the instrument itself. Carefully designed tests in the oscillatory mode permit study of solids or other elastic materials because the degree of the deformation (strain) can be kept to a minimal level (within the linear viscoelastic region) to preserve structure; this approach has been performed for several decades in the polymer/plastic fields. Another advantage of the oscillatory mode is that it allows elastic and "purely viscous" behavior to be differentiated. As described below, oscillatory rheology measures a complex shear modulus, G*, a resistance to deformation, and permits dissection of this stress into an elastic or storage modulus, G' and a viscous or loss modulus, G". Also described below is the relationship of the waves of stress *versus* that of strain during the oscillation. This type of rheometer also determines the degree to which the waves are out of phase as a phase angle. The degree of elasticity is reflected in the phase angle (or its tangent), δ, which is the phase lag between the wave forms of the shear stress and shear strain. In these studies, the shear moduli and the phase angle were useful tools for understanding events in the rubbery state of the frozen sample.

Focus of Paper

During our routine formulation development, several mAb formulations showed instability during frozen storage at ≥−30°C or freeze-thaw characterization. This paper describes a mAb that showed an increase in high molecular weight species (HMWS) upon storage at −10°C, but not at the other frozen temperatures tested (−15°C or −20°C) or the liquid stored at 4°C. All three frozen storage temperatures were above the Tg' values of the formulations as measured by DSC, meaning the protein was in a rubbery phase. However, the physical instability was only seen at −10°C. Between the Tg' and the final ice melt near 0°C, the DSC thermogram was devoid of transitional events. Since the instability could not be explained by the glassy or rubbery state of the freeze concentrate as determined by DSC, we employed oscillatory shear rheology, to more directly detect changes in the mechanical resistance to deformation to see if there was evidence of changes in the physical state/phase behavior in this temperature range above the Tg'. In this paper, the relationship between rheological properties, thermo-related phenomena (Tg') and physical stability of the protein in the frozen state is explored. To our knowledge, we report the first published application of oscillatory shear rheology as a noninvasive and highly sensitive tool to directly monitor phase behavior of antibody formulations in the frozen state and that can serve as a complement to other low temperature techniques.

MATERIALS AND METHODS

Materials

The IgG2 monoclonal antibody used in this study was produced at Amgen Inc. (Thousand Oaks, CA), at 70 mg/mL formulated with 10 mM sodium acetate (J.T. Baker, Phillipsburg, NJ) with 9% (*w/v*) sucrose (EMD, Gibbstown, NJ), pH 5.2.

Stability Studies

The antibody formulations were prepared at a protein concentration range of 10–160 mg/mL typically in formulation buffer (FB: 10 mM sodium acetate, pH 5.2, with 9% *w/v* sucrose and 0.004% *w/v* polysorbate 20). The low concentration samples of antibody were prepared by dilution from 70 mg/mL with its formulation buffer. The 160 mg/mL antibody formulation was prepared by concentration using centrifugal ultrafiltration.

The formulations were filtered through 0.22 μm filters, 1 mL of each solution was aliquoted into 3 cc glass vials and stored (capped and sealed) at 25°C, 4°C, −10°C, −15°C, −20°C and −30°C for periods of time up to 12 weeks. Note that samples stored at −10°C and −15°C directly (i.e., vials of liquid sample placed in the freezer without any pretreatment) do not always solidify. At −10°C, about half the samples will remain liquid. So the stability samples at −10°C and −15°C were first prestaged at −30°C for 24 h then moved to the −10°C and −15°C freezers, respectively. However, for one of the studies in the "Supercooled Formulations" section below, a batch of 10 vials was stored directly at the study temperature, with about half remaining liquid and half solidifying.. Samples were thawed at room temperature prior to analysis by SE-HPLC. If there was any leftover material in a timepoint, it was not reused.

Low Temperature Oscillatory Rheology

Background

For reasons discussed above, these studies were conducted in the oscillatory mode to obtain useful data on a rigid sample. The measurement configuration was a sandwich of the sample between two parallel plates, a bottom one that is stationary and an upper plate on a rotating shaft; this arrangement applies a defined stress to the sample surface and measures the resultant displacement. In an oscillatory measurement, the degree of the displacement is expressed as "strain", a dimensionless quantity which is the ratio of the displacement to the gap between the plates (thickness of the

sample). The upper plate turns a defined amount in one direction from an initial reference point, stops, returns through the reference point and to an equal displacement in the other direction, then back. G* is defined as the ratio of amplitudes of the whole shear stress wave to shear strain wave. During each experiment, the sample was loaded as a liquid, frozen to a nominal temperature of −40°C (calibrated temperature −46°C), then gradually heated, so that the material was ice for part of the experiment, thus very rigid, and required oscillatory testing at very low strain and frequency to avoid slippage or other instrument limitations.

Another reason for the use of the oscillatory method was to obtain information on both the elastic and viscous nature of the material. The shear modulus, G*, is a complex function of two components, G' and G": G*=G'+iG". G' is the energy stored in system where deformation is reversible; like a Hookean solid, or spring, this is proportional to the strain, which is the extent of deformation (24). G" measures the energy lost as frictional heat during an irreversible deformation; like a Newtonian fluid (24), this is proportional to the rate, not merely the extent of deformation. Note that the term viscosity has two senses, a broader meaning that encompasses all the resistances to movement in the G* and the narrower usage that applies to irreversible deformation that is reflected in the G". Regarding the broader meaning, there is a complex viscosity, η* that corresponds to the G*, where η*=G*/ω and ω is the angular velocity of the oscillation in radians/s. In terms of the typical viscosity measurement done under steady shear (in situations where what is known as the Cox-Merz rule (25) holds) η equals η* when the steady shear rate = ω. In oscillatory experiments, it is possible to measure both the G' and G" because the former responds to the extent of deformation while the latter responds to the rate of deformation. Because the stress for a purely elastic material is proportional to the strain, it is maximal when the strain is maximal, i.e., when the plate stops at the maximum displacement from the reference point, and it is minimal as it swings past the reference point on the way to the other extreme of the oscillation. Thus, the stress wave and the strain wave are in phase, the phase difference, or phase angle, δ, is zero. However, if the material has negligible elasticity and the resistance to flow is from friction, the stress is proportional to the rate of deformation, which is minimal when the plate stops at maximal strain and maximal as the plate swings past the reference point (zero strain). Thus, a totally "viscous" material will have a δ of 90° (1/4 of the 360° oscillation). Many materials are viscoelastic, having both viscous and elastic nature, with phase angles between 0° and 90°. An important relationship is G"/G' = tanδ, and when G" = G' (tanδ=1 and δ=45°) there is a crossover point between a predominantly viscous to predominantly elastic nature; tanδ can be also interpreted as the ratio of energy lost to energy stored per cycle.

Method of Rheology

Dynamic oscillatory rheology measurements were made using a rotational Rheometer (Gemini 200 HR Nano, Malvern Instruments, Massachusetts) equipped with a parallel-plate fixture (ETC25 parallel plates, 25 mm in diameter) and a temperature controller (Extended temperature cell, or "ETC.") connected with liquid nitrogen. All tests were oscillatory in the autostress mode (maximum stress, 3000 Pa) with a target strain of 0.1% and two iterations, at a single frequency, 0.2 Hertz. At 0.1% strain and a gap of 500 μm the plate movement was only 0.5 μm. Because the measurement cycle encompasses many decades of G*, care was taken to find a combination of frequency and strain that permitted measurement at low as well as high G*. At low G*, inertial effects can produce inaccurate and erratic data. Reducing the frequency to a very low level and using a small gap solved this problem. When measurements in the direct strain control mode were attempted on these samples, poor quality data was obtained: the signal to noise ratio was high, and the harmonic distortion of the waves was high. The autostress mode is a special form of stress control, where more than one stress is tested at each data point, until a target strain is achieved. At most data points, this was achieved in the two iterations, the sole exceptions being the initial point taken when a new test segment was begun after the sample was frozen. Since this point was clearly an outlier on the frozen plateau, it was discarded. Use of the autostress mode greatly improved the coherence of the wave forms.

Precautions were taken with regard to temperature. The thermal compensation feature was enabled to correct for dimensional changes in the parallel plates with temperature. Because the temperature sensor was embedded in the bottom plate (2–3 mm below the sample gap between the two plates), there was some difference between the measured temperature and the actual temperature of the sample above the plate. This could be observed in the heating curve of G* *versus* temperature for ice, where the drop in modulus occurred approximately 6°C above the known value of 0°C for the melting point of ice. This difference appeared to be the same throughout the temperature range in these studies, as confirmed by melting curves for a variety of salts at their eutectic concentrations (26,27). The rheometer temperatures were calibrated using known eutectic melting temperatures of different salt solutions (concentrations in % *w/w*; majority of the salts were obtained from Sigma Aldrich): 21.6% $MgCl_2$ (T_{eut}: −33.6°C), 40% NaBr (T_{eut}: −28.0°C), 23.3% NaCl (T_{eut}: −21.1°C), 38.3% $(NH_4)_2SO_4$ (T_{eut}: −19.1°C), 37% $NaNO_3$ (T_{eut}: −17.4°C), 19.8% KCl (T_{eut}: −11.1°C), 27.2% $ZnSO_4$ (T_{eut}: −6.6°C),and 19% $MgSO_4$ (T_{eut}: −3.9°C (27)). When the midpoints of the melting transitions were analyzed from the log G* *versus* temperature

plots, the average for all the examples was 6°C too high, with a standard deviation of 1°C. Therefore, temperatures reported here were adjusted by subtracting 6°C.

Approximately 0.3 mL liquid sample was loaded between the two parallel plates (upper plate, 25 mm diameter) with a gap of 0.5 mm at room temperature. A dynamic temperature sweep test with nominal temperature range from −40°C to +5°C was used for rheological measurements. The temperature profile was generally as follows: 1) the sample was first cooled to −40°C (nominal temperature—actual temperature −46°C) at a rate of 3°C /min, 2) held at this temperature for 5 min, and 3) then heated back to +5°C at a rate of 2°C/min, (ramp rates ranged from 1 to 4°C/min, but did not typically affect the results). The thermograms of only the heating cycle profiles are reported here. The Malvern software was used to obtain the rheological parameters, e.g. G* and δ. The onset softening (Ts*) was determined from the first drop in G* on linear y-axis temperature during the heating cycle. The upper limit of the shear modulus for the instrument was ~3 MPa due to the compliance of the upper fixture with this plate attached. Since rigid solids (e.g., steel, ice, minerals etc.) have a shear modulus (G*) in the GPa range (28–30), they cannot be accurately measured in this range and the G* and δ readings should be interpreted as apparent readings with the true G*>> 3 MPa. The modulus readings we report are the raw data and we did not employ any compliance correction and there is some possibility that Ts* could have been overestimated, so we did comparisons with Tg' to gauge the extent of any overestimate. This does not affect the interpretation of the data above Ts*, the temperature range of concern in this study because the data lie well below the limiting modulus.

The G* and δ were used to define an initial softening temperature, Ts*, as the onset of the softening event, that is, where the G* just began its decrease and δ its increase. This deviates from some procedures reported in the literature (31,32) where attempts were made to measure the Tg of polymers by dynamic mechanical methods. This literature has proposed three definitions of Tg: the onset of the decline of G* (or G') as taken from the midpoint of the transition, a peak that occurs in G", and a peak in tan δ. As the data below show, Ts* was greater than or equal to the Tg' measured by DSC. When these alternate methods were used the transition temperature was much higher. We opted for the lowest onset of the change because at the higher temperatures enough change may have occurred to cause protein instability. For example, the peak in the G" is attributed to there being sufficient motion in the system to generate a large increase of frictional heating.

Modulated Differential Scanning Calorimetry (MDSC)

Samples (ca. 10 to 20 μl) were hermetically sealed in aluminum pans and tested in a modulated DSC (studies were performed using a TA Q1000, 2920 MDSC (TA Instruments, Leatherhead, UK) equipped with a refrigerated cooling system. Dry nitrogen was used as the purge gas with a flow rate at 50 mL/min. Sealed solution samples in the DSC cell were first slowly cooled at 3°C/min to 0°C and held for 5 min to obtain isothermal equilibration to mimic the rheometer temperature profile. Then, the modulated DSC scan with amplitude of 0.5°C and a period of 100 s heated the sample at 0.5°C/min. Tg' was reported as onset and inflection points of transition steps.

Differential Scanning Calorimetry (DSC)

Sub-ambient thermal analysis was carried out on a Pyris 1 DSC (Perkin-Elmer Corp., Norwalk, CT) equipped with liquid nitrogen to cool to −120°C. Temperature calibration was performed (at a heating rate of 5°C/min) using the melting points of hexane (−95°C) and cyclohexane (6.5°C) standards. An empty sealed DSC pan was used as a reference. A standard built-in software method was used to determine glass transition temperatures (T_g') and the onset of eutectic melts: room temperature sample (40 μL) was loaded into a 50 μL semi-hermetically sealed DSC pan, which was then placed in the DSC cell. Samples were cooled to −70°C at a rate of 60°C/min, held at −70°C for five minutes before heating to +25°C at a rate of 5°C/minute. The baseline slopes were optimized and the glass transition temperatures were determined using the Pyris Thermal Analysis software for Windows version 3.81.

Estimation of Amount of Frozen Ice Using DSC

The amount of ice in the frozen formulation was estimated from the melting of the ice upon heating at 1.2°C/min using standard DSC mode. The heat of fusion was calculated from the integration of the endothermic peak corresponding to the melting of the ice ranging from the end of Tg' to the endset of the melting. Each sample was measured twice. Weight percentage of unfrozen water was calculated from the following equation,

$$H_2O_{unfrozen}\% = 100 - \text{ice}\% - \text{sucrose}\% - \text{protein}\% \quad (1)$$

where ice % is the weight percentage of ice, sucrose% is the weight percentage of sucrose (9%) and protein% is the weight percentage of protein. The freeze concentration was calculated from

$$\text{Freeze concentration} = [\text{Protein}]_{initial}/(100 - \text{ice}\%)*100 \quad (2)$$

where $[\text{Protein}]_{initial}$ is the initial protein concentration before freezing.

Size-Exclusion High Performance Liquid Chromatography (SE-HPLC)

Physical degradation of the protein such as the presence of soluble aggregates or clipped species was determined by SE-HPLC on an Agilent 1200 HPLC system equipped with Chromeleon software. The method employed one column (Tosoh G3000SWxl, 7.8 mm × 300 mm) at 25°C. Twenty eight micrograms of protein was loaded onto the column and eluted isocratically at a flow rate of 0.3 mL/min with a mobile phase consisting of 100 mM sodium phosphate and 300 mM sodium chloride, pH 6.8. The protein was monitored using UV detection at 235 and 280 nm. Peak areas in the chromatogram generated at 235 nm were used to quantify the amount of main peak (monomer), soluble high molecular weight species (HMWS aggregates or pre-peak) and low molecular weight species (clip or post peak). The precision of the method is less than 0.1% RSD for both main peak and pre-peak (n=4–5 for a standard of this protein and n=1–2 for sample at each time point).

RESULTS

IgG2 mAb Stability

This IgG2 mAb at 70 mg/mL in an isotonic sucrose formulation underwent an increased aggregation at −10°C that began as early as two weeks of storage and generally tracked with the HMWS data for the same formulation stored at +25°C (Figs. 1, 2). Figure 2 presents representative data from one of several temperature studies and shows that the other samples that were stored at −15°C, −20°C and −30°C (Fig. 2) showed no appreciable change, nor did a liquid control sample at 4°C (note that samples stored at −10°C and −15°C were first "pre-staged" at −30°C to ensure that they were solidified.). In Supplementary Material, Appendix I presents a detailed statistical evaluation of all the studies, which overall showed similar trends, in particular that the −10°C samples had more HMWS than the other frozen

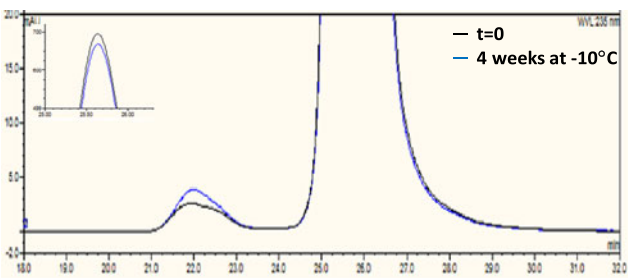

Fig. 1 Comparison of HMWS (pre-peak) for the IgG2 in FB stored at −10°C for 4 weeks *versus* a time zero sample. Inset shows main peak height. SEC chromatogram (intensity vs time).

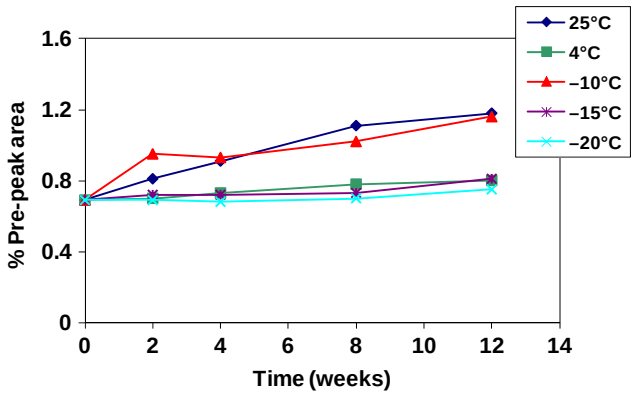

Fig. 2 Percent pre-peak area (HMWS) determined by SE-HPLC of the IgG2 at 70 mg/mL in FB as a function of storage temperature and time – a representative storage study (more in Supplementary Material, Appendix I).

samples after 12 weeks, and this difference was statistically significant. Other measures of stability (data not shown) including FTIR, near-UV CD and far-UV CD, did not indicate secondary or tertiary structural changes after 1 year of storage at 4°C, −10°C and −20°C. Figure 3 shows that aggregation decreased with decreased protein concentration at −10°C, and at the lowest protein concentrations, 20–30 mg/mL, samples were stable out to 12 weeks. At 40 mg/mL, there was some increased aggregation at −10°C (but not at −15°C and below), but much less than at 70 mg/mL.

DSC and MDSC Analysis

Figure 4a shows the total heat flow obtained from the MDSC was similar to the heat flow obtained from the conventional DSC for the frozen sucrose buffer with different amounts of the IgG2. The large endotherm near 0°C corresponds to the melting of the frozen sample, whose major component is ice. The temperature range between −60°C and −20°C is expanded and presented in the insert of Fig. 4a. The broad and weak baseline shift near −50°C

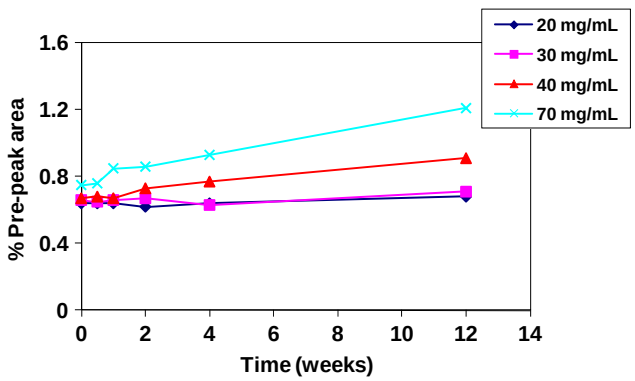

Fig. 3 Percent pre-peak area (HMWS) determined by SE-HPLC of the IgG2 formulated with FB as a function of protein concentration and storage time at −10°C.

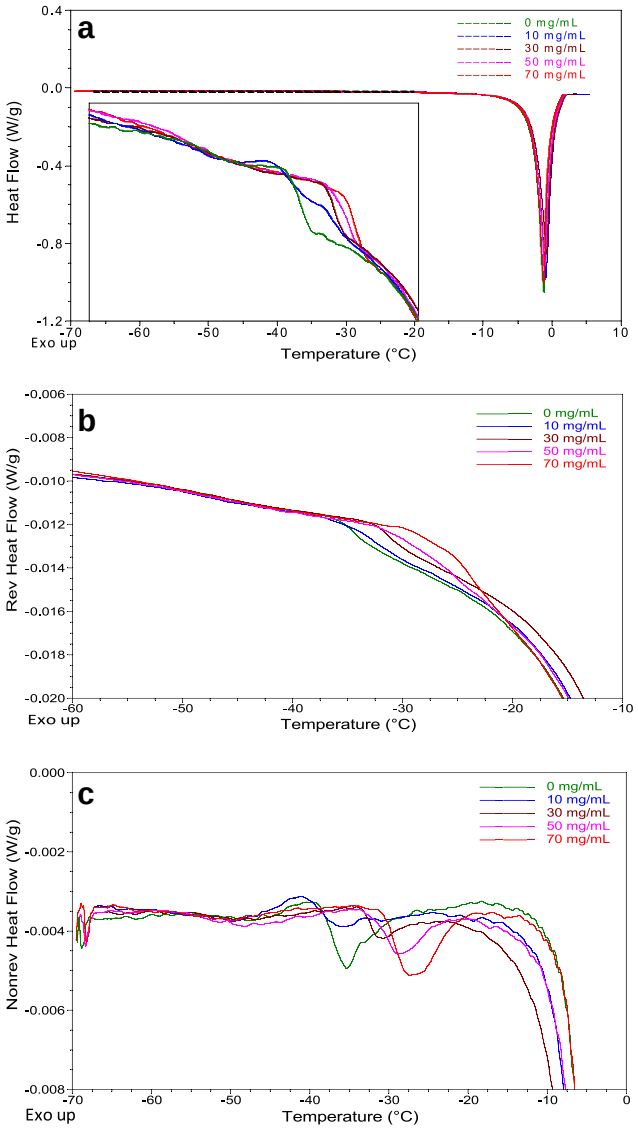

Fig. 4 Thermographs of different concentrations of the IgG2 in FB determined by MDSC: (**a**) top panel: total heating flow, inset: heat flow magnified 100-fold; (**b**) middle panel: reverse heat flow; (**c**) bottom panel: non-reverse heat flow.

corresponding to Tg" (the glass transition temperature of the amorphous sucrose solution, whose concentration lies between the nominal concentration of the given solution and the concentration of the maximally freeze-concentrated amorphous phase) (33,34) was resolved in the sucrose buffer without or with 10 mg/mL of the IgG2. The Tg" was followed by an exothermic shift, which is ascribed to the crystallization of non-equilibrium unfrozen water (33). A sharp baseline shift that tailed the exotherm represents Tg', whose endset overlaid with the onset of ice melting. In comparison, the increased protein amount in the sucrose buffer decreased the signal of Tg" and the exothermic water recrystallization peak, and also shifted the Tg' transition to a higher temperature range. Figure 4b shows the reversed heat flow of the corresponding samples in Fig. 4a. The Tg" values of all samples were slightly resolved and unchanged in terms of temperature. The increased protein amount in the sucrose buffer increased Tg', resolved using reversed heat flow, and the value of this Tg' was higher than that determined in total heat flow thermograms or using conventional DSC (35). Only the onset and inflection points of Tg' were determined because of the overlay of the endset of Tg' and onset of ice melting. Figure 4c shows non-reversed heat flow profiles of five samples, which presented two consecutive exothermic and endothermic peaks near the Tg' temperature range that correspond to the exothermic ice crystallization and possibly endothermic enthalpy recovery (33) or ice-dissolution (36). The amplitude of the endotherm appeared dependent on the protein concentration as indicated in Fig. 4c. For ease of comparison, the onset and midpoint/inflection points of Tg' for DSC and MDSC are summarized in Table I. For each concentration (except for the 30 mg/mL) the onset temperatures were within ~2°C of each other as were the midpoint/inflection points; this similarity gives added confidence in the values of Tg' by calorimetry.

Estimation of Amount of Frozen Ice Using DSC

The amount of ice in the frozen formulation was estimated from the melting of the ice using DSC. The results are shown in Table II. At −20°C, the percent ice varied from 79% to 70% when the protein concentration increased from 0 to 70 mg/mL. There was slightly higher percent ice in the samples at −20°C *versus* −10°C. With the 70 mg/mL protein sample, the components were concentrated ~2 to 3-fold at −10°C.

Oscillatory Rheology

Oscillatory measurement at extremely low deformation (the movement of the measurement plate was 0.5 μm in each direction) permitted us to track the changes of the G* during the melting of pure ice (Fig. 5). The observed shear modulus (resistance to deformation), G*, remained at the upper limit of the measuring system at ~3×10^6 Pa, then dropped precipitously, 6 orders of magnitude, near 0°C, the melting point. The corresponding phase angle, δ, was near zero for most of the range, which meant the stress and strain maxima were in synchrony, characteristic of an elastic material. As the melting point was approached, the δ rose near the maximum value of 90°, where the maximum stress lagged the strain, which implied that the resistance to deformation was now purely frictional rather than from any interconnected structure. Profiles similar to water were seen for melting of eutectic compositions of salts, except that the sharp melt occurred at the eutectic temperatures, not 0°C. The IgG2 at 46 mg/mL in dilute sodium acetate buffer (no

Table I Summary of the Tg' Values Determined by Both DSC and MDSC and Ts* Determined by Low Temperature Rheometry for the Corresponding IgG2 Concentrations in FB

Protein conc. (mg/mL)	Tg' (°C) DSC (onset)	Tg' (°C) DSC (midpoint)	Tg' (°C) MDSC (onset)	Tg' (°C) MDSC (Inflection point)	Ts* (°C)
0	−33.9	−32	−35.8	−34.3	−32
10	−34.9	−32.8	−34.1	−32.7	−31
20	–	–	–	–	−28
30	−30.2	−27.2	−32.6	−31.4	−25
40	–	–	–	–	−24
50	–	–	−30.4	−25.8	−22
70	−28.5	−24	−26.8	−23.9	−18

Note: Error estimate ~≤5% (n=2–4); MDSC cannot determine end point due to overlay of melting.

sucrose) melted similarly to water (Fig. 6), with a softening temperature, Ts* near −5°C. Other mAbs and bovine serum albumin in water, or dilute buffer, showed a similar pattern (data not shown) and a Tg' was not observed by DSC.

The placebo formulation exhibited very different behavior from the above examples, as shown in Fig. 8, and this profile is almost the same as the one for 9% sucrose in Fig. 7 (Note that Fig. 7 includes curves for other sucrose concentrations and these are discussed in Supplementary Material, Appendix II). Both melting curves featured two softening temperatures: a principal one near −32°C, which matches the literature Tg' for a maximally freeze-concentrated solution (33), and a secondary one at higher temperature, somewhat variable in the range of −5°C to −15°C, that preceded the water melt near 0°C. After the initial softening, beginning at Ts*, there was a partial rehardening, ~10-fold increase in G*, that began near −20°C, followed by a secondary softening (Ts2*) that began at the secondary G* peak near −15°C. The resulting dip in the G* profile was variable in magnitude. The secondary rehardening peak appeared to be the development of viscoelastic structure, as there was a pronounced drop in the phase angle, the significance of which will be discussed below. The shear modulus (G*) of these hardening and softening events, ~10^5 Pa to ~10^6 Pa is similar to that of synthetic rubbers (37) and hard dairy products such as cooled butter (38) or aged cheese (39). In addition to G*, Fig. 8 compares different estimates of the temperature transition, T, for the placebo formulation. These literature methods were mentioned above and those results are discussed in Supplementary Material, Appendix III.

The Ts* changed upon addition of protein, and rose with increased protein concentration. The presence of the IgG2 at 70 mg/mL raised the Ts* to about −18°C (Fig. 9); this was near the Ts2* of the 9% sucrose buffer (Fig. 8). Figures 10 and 11 show the effect of protein concentration on the G*, δ, G" and G' as a function of temperature. The Ts* and Ts2*, for protein concentrations of 40 mg/mL and below, occurred at temperatures lower than those for 70 mg/mL but higher than the Tg' of sucrose solutions without protein. Some interesting features in the rheological profile were the changes in δ. For the 20 mg/mL formulation at temperatures between −16°C and −13°C, δ dropped indicating the possible development of gel structure, but began to rise again at approximately −13°C and warmer. However, for the 40 mg/mL solution there was a continuous increase of δ when heated from approximately −25°C to about −5°C with only a minor dip in δ (at~−12°C) (the angle is well above 45°). The 70 mg/mL sample showed a continuous rise in δ above approximately −20°C and the G* at −10°C was lower than the other samples.

Table II Percentage Ice and Freeze Concentration Factor Determined by DSC for IgG2 in FB

Protein conc. (mg/mL)	−20°C		−10°C	
	Ice %	Freeze conc. (fold)	Ice %	Freeze conc. (fold)
0	79	~5	77	~4
10	79	~5	76	~4
30	73	~3.7	71	~3.4
50	73	~3.7	71	~3.4
70	70	~3.3	67	~3

Note: error estimate ~≤5% (n=2)

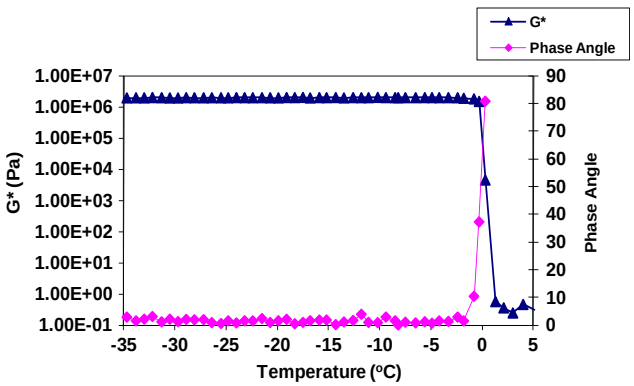

Fig. 5 Rheological profiles (G* and phase angle) of water as a function of temperature.

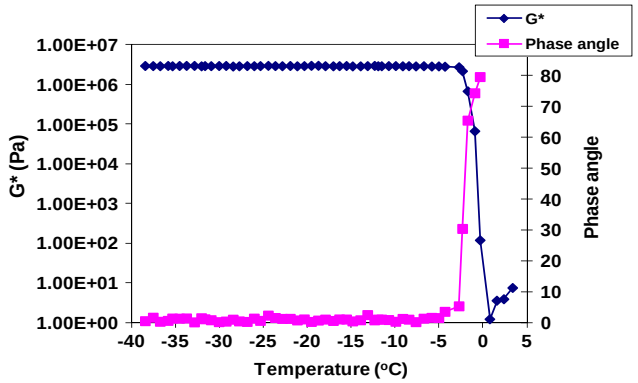

Fig. 6 Rheological profiles (G* and phase angle) of the IgG2 at 46 mg/mL formulated with 10 mM sodium acetate, pH 5.2 as a function of temperature.

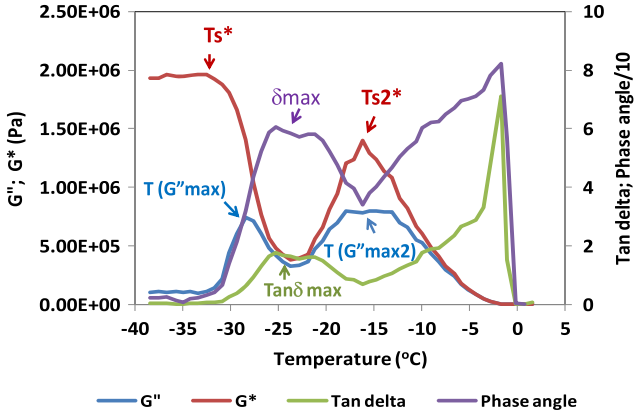

Fig. 8 Rheological profiles of G*, G", tanδ and phase angle of FB formulation buffer in the absence of protein as a function of temperature.

Table I shows a summary of the Tg' values for both DSC and MDSC as well as Ts* for the corresponding protein concentrations. Where the protein concentration was low (10 mg/mL) or zero. Ts* was close to −32°C, the literature Tg* for sucrose solutions, and the DSC midpoint reported here. In these instances the 3 MPa limit for the instrument did not appear to cause a major overestimation of Ts*, on the assumption that it should be the same as Tg'. With higher protein concentration both the Tg' and Ts* values increased, but the the Ts* was higher than Tg' by DSC. We cannot be certain whether the Ts* was higher because of the 3 MPa limit, or because it actually was different. As discussed below, the key rheological changes that are associated with reduced protein stability occur above Ts*, where the G* was on scale. As discussed in Supplementary Material, Appendix III, the T(G"max) and T(tanδmax) were much larger than the Tg' by DSC.

Supercooled Formulations

Supercooling was exploited to discern the effects of cold concentration, ice-water interface and cold denaturation.

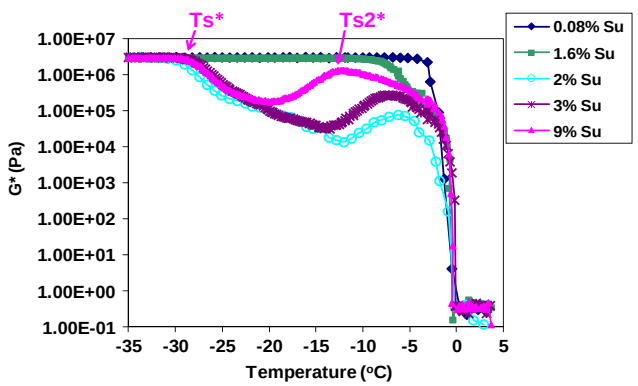

Fig. 7 Rheological profiles (G*) of sucrose solution in water as a function of temperature and sucrose concentration.

Cold concentration was simulated by concentrating the 70 mg/mL protein formulation in the 3-fold range, the level of concentration indicated by ice analysis (Table II). Specifically, a stability study was performed on 2.3-fold concentrated protein (160 mg/mL) in a 3-fold concentrated buffer (30 mM acetate buffer and 27% sucrose, pH 5.2). After direct storage for one month (no prestaging) at −10°C, −15°C and −20°C, all the samples were frozen, except for those samples at −10°C which supercooled and remained liquid. All of the super-cooled samples stored at −10°C showed no degradation by SE-HPLC analysis after the one-month duration of the study (data not shown).

For formulations at the 70 mg/mL concentration in FB, individual samples stored directly at −10°C vary as to whether they freeze or remain liquid because of the stochastic nature of supercooling. Figure 12 compares the stability of liquid and frozen 70 mg/mL IgG2 in FB at −10°C by SE-HPLC. The liquid samples, which were simply exposed to cold temperature, without ice-water interfaces, were stable; where ice was present, aggregation occurred.

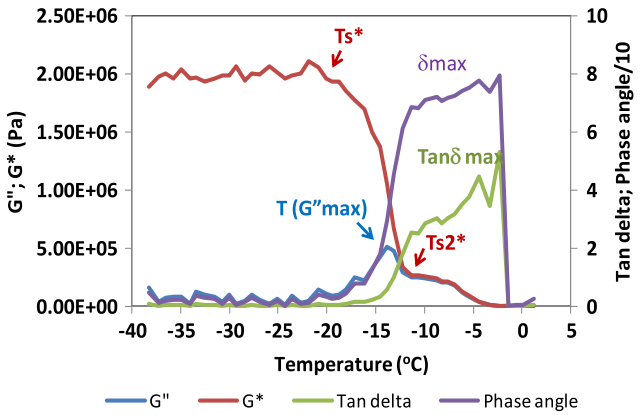

Fig. 9 Rheological profiles of the IgG2 at 70 mg/mL formulated with FB as a function of temperature.

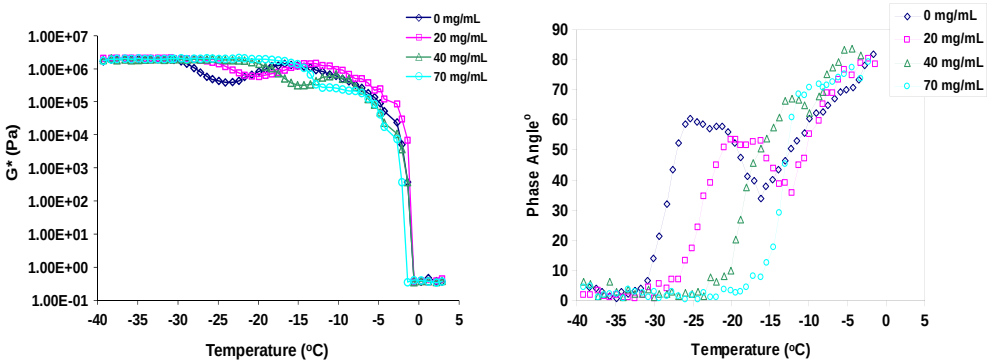

Fig. 10 Rheological profiles (G*- left panel and phase angle- right panel) of the IgG2 formulated with FB as a function of protein concentration and temperature.

DISCUSSION

In these studies, we sought a greater understanding of the frozen state by rheological study of a particular sucrose-based protein formulation with a puzzling frozen stability profile. There are two main aspects to this paper: 1) stability studies of the protein formulation to elucidate the circumstances where HMWS occurred and 2) rheological study of the softening/hardening events in the temperature range in question. Below, the relationship between the stability and the rheology is explored.

Frozen State and Protein Stability

During frozen storage above the Tg', this IgG2 mAb at 70 mg/mL in a sucrose-containing formulation developed HMWS at one of the study temperatures, −10°C, but not at the others, -15°C and −20°C. At −10°C, comparison of supercooled *versus* frozen samples indicated that ice exposure likely caused the instability, and not simply cold denaturation. However, ice was also present at the other two temperatures where the formulation was stable. This demonstrated that not all "frozen" samples were equivalent, and the difference was likely in the state of the freeze concentrate despite the absence of thermal events in this temperature range as determined by DSC.

Considerable literature (e.g., (40)) advocates frozen storage in a glassy state. To prevent ice/liquid interface denaturation, this approach keeps the formulation cold enough to effectively immobilize the protein and thus slow the time-scale of interaction with ice surfaces. As discussed above, when a sucrose solution freezes, the sucrose freeze-concentrates, until the temperature reaches the Tg', where the concentrate is so viscous that it essentially immobilizes all the molecules, even water. The frozen state of this type of formulation (below Tg') may be thought of as a mosaic of a crystalline ice phase with an amorphous sucrose-protein mixture filling the interstices between the ice grains (Fig. 13). This concept is supported by the recent report of Dong *et al.* where Raman confocal freeze dry microscopy was used to study trehalose-protein solutions (trehalose also freeze concentrates) (17). Dong reported that the protein was mainly located in the freeze concentrate though some was associated with the ice grains. Stability indicators such as the α-helix content indicated that the protein in these interstices was largely in the native state, while a small population of protein molecules associated with the ice grains was denatured. Figure 13 schematically summarizes

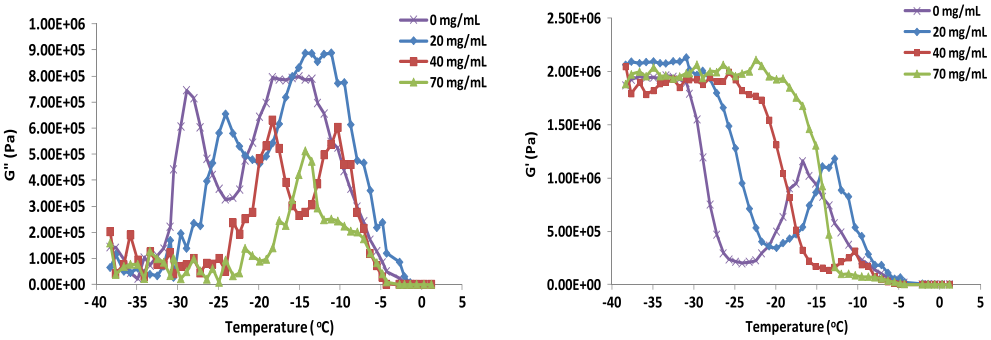

Fig. 11 Linear plots of G" (left panel) and G' (right panel) for the IgG2 formulated with FB as a function of protein concentration and temperature.

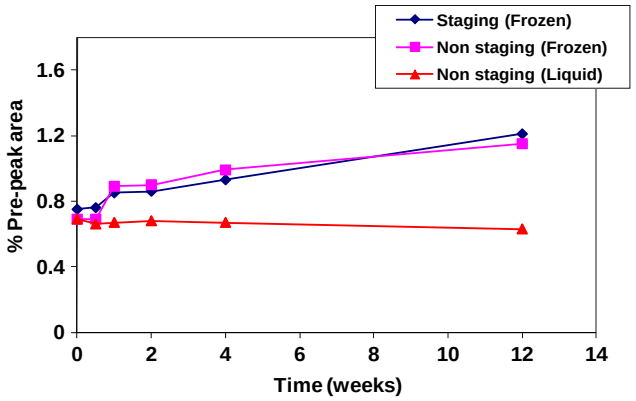

Fig. 12 Percent pre-peak area (HMWS) determined by SE-HPLC of the IgG2 70 mg/mL formulated in FB after storage at −10°C with pre-staging (frozen form) and without pre-staging (both liquid and frozen form) as a function of storage time.

what possibly is happening when a glassy, frozen formulation is heated. We refer to this representation as the Frozen Mosaic Model; other recent literature shows similar representations of the frozen state (17,18,41,42).

According to the Frozen Mosaic Model, the Tg' event is in the amorphous region between the crystalline ice blocks. At Ts*, the oscillatory stress allows movement between the ice blocks and there is also enhanced protein mobility. At higher temperatures there is melting of the ice blocks. Diffusion calculations of molecular movement and spacing (see Supplementary Material, Appendix IV) indicate that collisions between the mAb molecules at −10°C are likely high during the time scale of our experiments. This is in contrast to the prediction at, for example, −30°C where the molecules move less than a few nm in the time scale of our studies. However, the multiple collisions at −10°C would occur whether there is ice present or not at similar protein concentrations, but we do not see instability with 2.3-fold concentrated samples that were supercooled and remained as a liquid at −10°C. The initiation of aggregation appears to result from the protein molecules hitting the ice wall of the channels (in Dong's paper, these are on the order of 10 μm across) and possibly becoming anchored and reactive through multiple hydrogen bonding sites to ice. The surface-immobilized protein molecule would then be a stationary target receiving numerous impacts from its protein neighbors. At temperatures lower than −10°C, the increase in viscosity and decrease in protein kinetic energy would diminish the effects of collisions and enhance stability.

There is a noteworthy similarity between the increase in HMWS at −10°C and at 25°C and perhaps the root of this is that the mechanisms in both cases involve collisions. At the lower temperature, we can hypothesize that ice acts as a catalyst lowering the activation energy for aggregate formation (perhaps including protein unfolding); in addition, one could certainly speculate about the relative contributions of the exponential and pre-exponential (energy) factors to the reaction rate using Arrhenius or Eyring-type equations, but this is beyond the scope of the current paper.

Above, we interpret the stability results in terms of the rheology of the rubbery freeze concentrate, but alternative explanations in terms of the size and morphology of the ice grains are possible. If the size of the grains were reduced at higher protein concentration, the ice surface area would thereby increase and thus the probability of protein damage by ice denaturation. DSC data indicates that the ice concentration declines with rising protein levels, but the size of the grains and change in ice surface is a topic for future work. Whether the rheology data could be interpreted as complex suspension behavior is another question.

Techniques to Measure Softening/Hardening Events

This study shows that rheological measurements can detect changes in the frozen mosaic between the Tg' and final melt, where no events were measured by DSC. It should be generally noted that the Tg of polymeric/plastic materials has been analyzed for decades using both DSC and oscillatory rheology and the results compared and contrasted; to the authors' knowledge, Tg is much less discussed using rheology in the pharmaceutical field. The

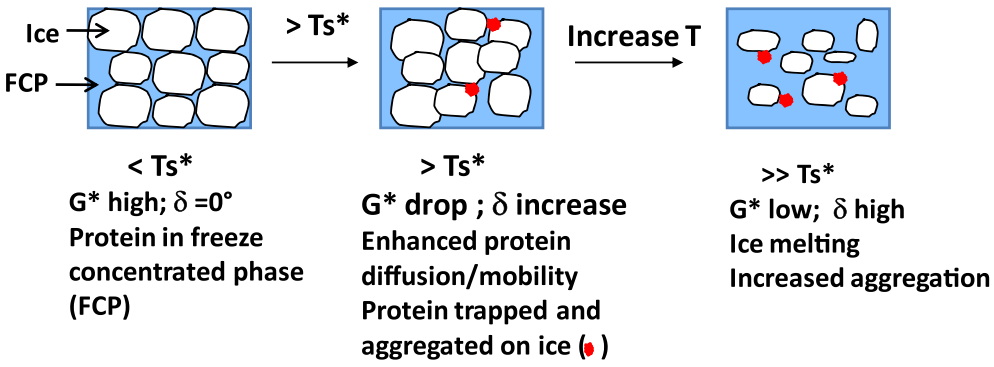

Fig. 13 Frozen mosaic model.

determination of the Tg by dynamic mechanical means is the subject of the test method ASTM E1640-09 (published 10/2009)(31); here the assignment of Tg as the onset of the drop of G' or the maxima in G" and tanδ are discussed. The literature has examples where the two techniques match and other cases where they differ greatly and authors have disputed whether there should be any correlation between the techniques (43–46). Calorimetry and rheometry measure fundamentally different processes. Calorimetry is sensitive to thermal changes caused by coordinated movement of molecules and/or their segments (47). Rheometry measures the stress on the system affecting molecules separated by several hundred nanometers and greater. We are interested in the point of overall softening of the formulation (as represented by G* or δ) and not assignment of a rheological Tg. We use Ts* as an empirical index of softening. The ease of large scale movement after Ts* signals a large increase of protein diffusion where over time the protein can travel the distance necessary to collide with another protein or with the ice/water interface where denaturation and aggregation events can occur.

Rheology of Frozen Sucrose Solutions

Our rheological studies showed that sucrose solutions exhibited melting behavior very different from water, eutectic salt solutions and protein in dilute buffer, which all softened rapidly abruptly at a melting point. Sucrose solutions of 2 to 9%, or the formulation buffer (9% sucrose, primarily), do not simply soften in a gradual way, either. Instead, there was a rehardening event after the Ts*, then a secondary softening at the Ts2*. For solutions in this concentration range, the Ts* was very close to the calorimetric Tg', but the rehardening and Ts2* occurred in the rubbery temperature range, where the DSC scan was essentially featureless. The "dip" appearing in the G* was somewhat variable in the temperature and magnitude. This may be due to softening assisted by dilution of the freeze concentrate by newly freed non-equilibrium water that was trapped in the glass – this would not be expected to be a strictly reproducible phenomenon. At temperatures just above the dip, the partial rehardening was accompanied by a drop in phase angle to a level consistent with elastic structure or gel formation (<45°). This general profile was typical of sucrose solutions down to 2% (*w*/*v*); see Supplementary Material, Appendix II for further discussion of dilute sucrose solutions.

Rheology and Stability of Frozen Protein/Sucrose Formulations

The presence of protein in the 9% sucrose formulation shifted Ts* higher than the placebo in a concentration dependent fashion until, at 70 mg/mL, Ts* was close to the Ts2* of sucrose alone. There was also no secondary rehardening and drop in phase angle, possibly because the sucrose was not free to associate with itself and form a structure. The rehardening and Ts2* were restored at protein concentrations ≤40 mg/mL, where the G* profile resembled that of the sucrose-only solutions except for the increase in Ts*. Unlike a sucrose formulation without protein, Tg' also rose with protein concentration, such that the protein-sucrose combination formed a more stable glass than sucrose alone. For the higher protein concentrations (>10 mg/mL), Tg' was significantly less than Ts*. As discussed above, rheological and calorimetric values of Tg' may be expected to differ and Ts* is not necessarily intended to equal the rheological Tg'. Although higher than the Tg', Ts* and perhaps the Ts2* still underestimated the temperature where stability was lost, so caution is needed in pinpointing destabilizing conditions based on this data. All of the protein formulations had values of Ts* below −15°C, a temperature at which all of them were stable. In fact, the lower the concentration (e.g., 20 mg/mL), the lower the Ts*, so strictly on the basis of Ts*, the lower concentration would have been expected to have the worst stability. In fact, just the reverse was true, and this was not surprising because lower aggregation often results from lower protein concentration since the collision frequency is reduced. However the trends in the phase angle were more predictive of stability than Ts*, and may help explain the stability profile. The 20 mg/mL had the lowest HMWS, 70 mg/mL the highest, and 40 mg/mL was between these. For both 20 and 40 mg/mL, the Ts2* was near −10°C, but the phase angle indicated possible gel structure at 20 mg/mL, but not at 40 mg/mL (only a slight dip in δ); 70 mg/mL exhibited no drop in δ above Ts*. Where there was evidence of more gel-like system, there was more stability. Thus, the secondary hardening event, with the development of a viscoelastic gel that immobilized the protein, appeared related to the diminished protein aggregation.

This viscoelastic gel is likely composed of an H-bonded network of sucrose molecules, and protein may compete with this gelation by binding sucrose. The absence of a gel may mean that the protein-sucrose interaction has bound up sucrose to the extent that there is insufficient sucrose to form the gel. Since the gel may help immobilize and stabilize the protein, loss of the gel may be one mechanism of the instability. Lack of a gel may also indicate that there is not enough sucrose to fully saturate protein-sucrose interaction sites and stabilization from sucrose binding may be reduced. At low protein concentration, the sucrose completely surrounds and protects the protein and stabilizes it and, in addition, there is sufficient excess sucrose to form the gel. This suggests preferential sucrose solvation to the protein and not the published "exclusion" mechanism (48–50) of sucrose; it should be noted however that the "exclusion" mechanism was thermodynamically modeled for fluids near ambient conditions and has not been proven to be relevant to the frozen state. Moreover, Timasheff *et al.* (48) showed that 20% sorbitol (4x isotonic) becomes preferentially bound

to native protein; in our case the sucrose is 3X concentrated in the frozen state so perhaps it also becomes preferentially bound. As the concentration of protein increases, the protein-sucrose combination in the freeze concentrate has an increased Tg' as a result of the weighted sum of the Tg' values as predicted by the Gordon-Taylor equation (51). Also, increased protein concentration likely causes significant protein/protein interaction which displaces the bound sucrose. This can result in pockets of free sucrose remaining in the protein assemblies that formed and may also explain the increased enthalpy recovery values measured by MDSC.

While rheology provided insights into changes in the rubbery state, DSC should be conducted along with oscillatory rheology to enhance the understanding of the frozen state where thermal events do not show up in the rheological measurement, such as the exotherm and endotherm near the Tg'. An example where this was imperative was for mannitol-containing formulation, which crystallizes near 0° C, and has a rheological profile similar to water (data not shown). The formulation is very stiff, but the mannitol no longer is available to protect the protein (40).

Practical Implications

Ts* and Ts2* are of practical interest in the selection of storage temperatures for frozen liquid formulations and perhaps shelf temperatures during lyophilization. These temperatures delineate a temperature range in which various softening and hardening events occur in the rubbery freeze concentrate, including possible formation of a gel-like entity by the sucrose, when the protein concentration is low enough. Formation of this entity is reflected by a decrease in the δ, and a distinct minimum in the δ below 45° may be a predictor of stability. However, with formulations where excipients precipitate, this may not hold (This will be discussed in a future publication with a sorbitol formulation; there is also a recent article (52) with a trehalose formulation). In characterizing the stability of protein formulations, it is important to select temperatures above and below Ts* and Ts2* temperatures to see if the particular system is sensitive to presumed ice denaturation; in the absence of the minimum of δ, more study temperatures should be tested. Detailed knowledge of the temperature-stability profile may also be needed in cases of freezer instability or failure during protein formulation storage, putting stability studies at risk. In addition to the mAb studied here, several other protein drug candidates have shown similar frozen temperature sensitivity (data not shown).

CONCLUSION

In the frozen state, immobilization of the solutes is a key to stability, whether to protect the stability of a protein as a frozen liquid or preserve the integrity of a nascent lyophilized cake. The temperature needed to achieve this has been thought to be less than the Tg' for frozen formulations. In our study of frozen liquid formulations, we found a complex temperature-stability profile and that the protein was stable at certain temperatures well above the Tg'.

Low temperature rheology proved useful in studying this case because it was able to detect changes in the formulation between the Tg' and the final ice melt (this is relevant because the IgG2 was unstable at −10°C). Unlike some alternative techniques, measurements are performed directly on undiluted sample. While DSC and MDSC can detect thermal behavior associated with crystallization, enthalpy recovery and glass transitions, in this case, no distinct events were seen between the Tg' and the final ice melt. But rheology showed the softening event, Ts*, could be well above the Tg' when protein was present. In the more dilute protein formulations, the rheological profile of the sucrose stabilizer dominated, Ts* was close to Tg' and a secondary softening/hardening process occurred (denoted as Ts2*). As protein concentration rose from 40 to 70 mg/mL, the resemblance to the sucrose-alone rheological profile was lost, and the secondary hardening event faded as Ts* rose well above the Tg'. The reduction in stability was also associated with a loss of gel-like character in the formulation. In this study, low temperature rheology had more direct use than DSC in explaining the stability results. However, other formulations, such as those where solute crystallization may occur, can require DSC as well as low temperature rheology to explain the stability behavior (subject of a future publication). Low temperature rheology may be a useful tool for characterization of lyophilization cycles and the influence of excipient compositions. Some investigators (53) have shown that the collapse temperature may be well above the Tg' and thus there would be an economic incentive to lyophilize above the Tg'.

Future work will also focus on refining the Frozen Mosaic Model (and its accompanying diffusional characteristics) to help better understand freeze/thaw behavior where protein instability is known to occur, for example by using orthogonal techniques (e.g., microscopic methods) to determine ice grain geometries as a function of freezing rates and storage conditions. In addition, geometrical effects of the sample placement in the rheometer cell, to better simulate actual cases of interest (vials, large containers etc.), would be an area worth exploring.

ACKNOWLEDGMENTS AND DISCLOSURES

We wish to thank the following individuals for their contributions to this work: Dave Brems, Susan Hershenson, Yijia Jiang, Cynthia Li, Jenny Li, Tiansheng Li, Xichdao Nguyen, Rulin Qian, Margaret Ricci and Philip Rolfe.

REFERENCES

1. Royand I, Gupta MN. Freeze-drying of proteins: some emerging concerns. Biotechnol Appl Biochem. 2004;39:165–77.
2. Bhatnagar BS, Bogner RH, Pikal MJ. Protein stability during freezing: separation of stresses and mechanisms of protein stabilization. Pharm Dev Technol. 2007;12:505–23.
3. Blondand G, Meste, ML. Principles of frozen storage. In: Hui YH, Cornillon P, Legaretta IG, Lim MH, Murrell KD, Nip WK, editors. Handbook of frozen foods. 2004. p. 13–54.
4. Privalov PL. Cold denaturation of proteins. Crit Rev Biochem Mol Biol. 1990;25:281–305.
5. Hansen A, Jensen MH, Sneppen K, Zocchi G. Hot and cold denaturation of proteins: critical aspects. Eur Phys J B. 1999;10:193–6.
6. Tangand X, Pikal MJ. The effect of stabilizers and denaturants on the cold denaturation temperatures of proteins and implications for freeze-drying. Pharm Res. 2005;22:1167–75.
7. Strambiniand GB, Gonnelli M. Protein stability in ice. Biophys J. 2007;92:2131–8.
8. Chang BS, Kendrick BS, Carpenter JF. Surface-induced denaturation of proteins during freezing and its inhibition by surfactants. J Pharm Sci. 1996;85:1325–30.
9. Strambiniand GB, Gabellieri E. Proteins in frozen solutions: evidence of ice-induced partial unfolding. Biophys J. 1996;70:971–6.
10. Gabellieriand E, Strambini GB. ANS fluorescence detects widespread perturbations of protein tertiary structure in ice. Biophys J. 2006;90:3239–45.
11. Piedmonte DM, Summers C, McAuley A, Karamujic L, Ratnaswamy G. Sorbitol crystallization can lead to protein aggregation in frozen protein formulations. Pharm Res. 2007;24:136–46.
12. Muraseand N, Franks F. Salt precipitation during the freeze-concentration of phosphate buffer solutions. Biophys Chem. 1989;34:293–300.
13. Meister E, Sasic S, Gieseler H. Freeze-dry microscopy: impact of nucleation temperature and excipient concentration on collapse temperature data. AAPS PharmSciTech. 2009;10:582–8.
14. Lucas T, Mariette F, Dominiawsyk S, Le Ray D. Water, ice and sucrose behavior in frozen sucrose-protein solutions as studied by 1H NMR. Food Chem. 2003;84:77–89.
15. Sahagianand ME, Goff HD. Thermal, mechanical and molecular relaxation properties of stabilized sucrose solutions at sub-zero temperatures. Food Res Int. 1995;28:1–8.
16. Varshney DB, Sundaramurthi P, Kumar S, Shalaev EY, Kang S-W, Gatlin LA, *et al.* Phase transitions in frozen systems and during freeze-drying: quantification using synchrotron X-Ray diffractometry. Pharm Res. 2009;26:1596–606.
17. Dong J, Hubel A, Bischof JC, Aksan A. Freezing-induced phase separation and spatial microheterogeneity in protein solutions. J Phys Chem B. 2009;113:10081–7.
18. Schwegman JJ, Carpenter JF, Nail SL. Evidence of partial unfolding of proteins at the ice/freeze-concentrate interface by infrared microscopy. J Pharm Sci. 2009;98:3239–46.
19. Blond G, Ivanova K, Simatos D. Reliability of dynamic mechanical thermal analyses (DMTA) for the study of frozen aqueous systems. J Rheol (N Y). 1994;38:1693–703.
20. Laaksonenand TJ, Roos YH. Thermal and dynamic-mechanical properties of frozen wheat doughs with added sucrose, NaCl, ascorbic acid, and their mixtures. Int J Food Prop. 2001;4:201–13.
21. Changand BS, Randall CS. Use of subambient thermal analysis to optimize protein lyophilization. Cryobiology. 1992;29:632–56.
22. Herrera JJ, Pastoriza L, Sampedro G. A DSC study on the effects of various maltodextrins and sucrose on protein changes in frozen-stored minced blue whiting muscle. J Sci Food Agric. 2001;81:377–84.
23. Saeedand S, Howell NK. Rheological and differential scanning calorimetry studies on structural and textural changes in frozen Atlantic mackerel (Scomber scombrus). J Sci Food Agric. 2004;84:1216–22.
24. Schoff CK. Rheological measurements. In: Mark H, Bikales N, Overberger V, Menges G, Kroschwitz J, editors. Encyclopedia of polymer science and engineering, vol. 14. New York: John Wiley and Sons; 1988. p. 454–541.
25. Larson RG. The Structure and Rheology of Complex Fluids. 1999.
26. Dean J. Lange's Handbook of chemistry, McGraw-Hill. 1999.
27. Van Der Ham F, De Graauw J, Seckler MM, Verdoes D, Witkamp GJ. Application of eutectic freeze crystallization to process streams and wastewater purification. NPT Procestechnol. 2001;8:14–9.
28. Crandall SH, Dahl NC, Lander TS. An Introduction to the Mechanics of Solids, McGraw-Hill. 1999.
29. Modulus of rigidity of some common materials. The engineering toolbox. http://www.engineeringtoolbox.com/modulus-rigidity-d_946.html.
30. Stevens H. Viscoelastic properties of frozen soil under vibratory loads. Permafrost, National Academy of Sciences, 1973. p. 400–9.
31. ASTM. Standard Test Method for Assignment of the Glass Transition Temperature by Dynamic Mechanical Analysis, Vol. E1640-09. doi:10.1520/E1640-09, ASTM International, West Conshohocken, PA, 2009.
32. Shawand MT, MacKnight WJ. Introduction to polymer viscoelasticity. New York: John Wiley & Sons; 2005.
33. Chang L, Milton N, Rigsbee D, Mishra DS, Tang X, Thomas LC, *et al.* Using modulated DSC to investigate the origin of multiple thermal transitions in frozen 10% sucrose solutions. Thermochim Acta. 2006;444:141–7.
34. Sikora A, Dupanov VO, Kratochvil J, Zamecnik J. Transitions in aqueous solutions of sucrose at subzero temperatures. J Macromol Sci, Part B: Phys. 2007;46:71–85.
35. Craig D, Barsnes M, Royall P, Kett V. An evaluation of the Use of modulated temperature DSC as a means of assessing the relaxation behaviour of amorphous lactose. Pharm Res. 2000;17:696–700.
36. Izard MJ, Ablett S, Lillford PJ, Hill VL, Groves IE. A modulated differential scanning calorimetric study. J Therm Anal Calorim. 1996;47:1407–18.
37. Summer JG. Engineered rubber products, indroduction to design, Manufacture and Testing, Hanser, Cincinnati, Ohio, 2009. p. 3–4.
38. Shuklaand A, Rizvi SSH. Viscoelastic properties of butter. J Food Sci. 1995;60:902–5.
39. Akand MM, Gunasekaran S. Dynamic rheological properties of mozzarella cheese during refrigerated storage. J Food Sci. 1996;61:566–8.
40. Carpenter JF, Pikal MJ, Chang BS, Randolph TW. Rational design of stable lyophilized protein formulations: some practical advice. Pharm Res. 1997;14:969–75.
41. Floresand AA, Goff HD. Ice crystal size distributions in dynamically frozen model solutions and ice cream as affected by stabilizers. J Dairy Sci. 1999;82:1399–407.
42. Singh SK, Kolhe P, Wang W, Nema S. Large-scale freezing of biologics A practitioner's review, part one: fundamental aspects. BioProcess Int. 2009;7:32, 34, 36, 38, 40, 42, 44.
43. Kasapis S, Al-Marhoobi IM, Mitchell JR. Testing the validity of comparisons between the rheological and the calorimetric glass transition temperatures. Carbohydr Res. 2003;338:787–94.
44. Cocero AM, Kokini JL. The study of the glass transition of glutenin using small amplitude oscillatory rheological measurements and differential scanning calorimetry. Journal of Rheology (New York, NY, United States). 1991;35:257–70.
45. Wu J, Reading M, Craig DQM. Application of calorimetry, Sub-ambient atomic force microscopy and dynamic mechanical analysis

to the study of frozen aqueous trehalose solutions. Pharm Res. 2008;25:1396–404.
46. Maurice TJ, Asher YJ, Thomson S. Thermomechanical analysis of frozen aqueous systems. In: Levineand H, Slade L, editors. Water relationship in food. NY: Plenum Press; 1991.
47. Angell CA. Relaxation in liquids, polymers and plastic crystals - strong/fragile patterns and problems. J Non-Crystalline Solids. 1991;131–133 (Part I):13–31.
48. Xieand G, Timasheff SN. Mechanism of the stabilization of ribonuclease A by sorbitol: preferential hydration is greater for the denatured than for the native protein. Protein Sci. 1997;6:211–21.
49. Changand L, Pikal MJ. Mechanisms of protein stabilization in the solid state. J Pharm Sci. 2009;98:2886–908.
50. Timasheff SN. Protein hydration, thermodynamic binding, and preferential hydration. Biochemistry. 2002;41:13473–82.
51. Gordonand M, Taylor JS. Ideal copolymers and the second-order transitions of synthetic rubbers. I. Noncrystalline copolymers. J Appl Chem. 1952;2:493–500.
52. Singh SK, Kolhe P, Mehta AP, Chico SC, Lary AL, Huang M. Frozen state storage instability of a monoclonal antibody: aggregation as a consequence of trehalose crystallization and protein unfolding. Pharm Res. 2011;28:873–85.
53. Meisterand E, Gieseler H. Freeze-dry microscopy of protein/sugar mixtures: drying behavior, interpretation of collapse temperatures and a comparison to corresponding glass transition data. J Pharm Sci. 2009;98:3072–87.